



AIAA 90-0280

**Pressure Drag Calculations on Axisymmetric
Bodies of Arbitrary Moldline**

B. Drew and A. Jenn

McDonnell Douglas Missile Systems

St. Louis, MO

28th Aerospace Sciences Meeting

January 8-11, 1990/Reno, Nevada

PRESSURE DRAG CALCULATIONS ON AXISYMMETRIC BODIES OF ARBITRARY MOLDLINE

B. K. Drew* and A. A. Jenn**

McDonnell Douglas Missile Systems Company
St. Louis, Missouri

ABSTRACT

A computer program has been developed to calculate pressure drag on axisymmetric bodies with arbitrary moldlines. The program is valid at subsonic, transonic and supersonic Mach numbers. Subsonic pressure drag is calculated by correlating skin friction and total body fineness ratio. Supersonic wave drag is determined using a numerical application of Whitcomb's area rule. The transonic drag rise is characterized using a polynomial curve fit between the subsonic and supersonic methods. The overall logic, capabilities, and limitations of the code along with experimental data comparisons are presented. The stand alone code is simple to use and can easily be implemented as a subroutine in Missile Datcom. The minimal run time enhances the codes' usefulness as a preliminary design tool.

NOMENCLATURE

a_n	= Fourier coefficients
$C_{D_{p_0}}$	= subsonic form drag
C_{D_w}	= supersonic pressure (wave) drag
C_f	= skin friction coefficient
C_p	= pressure coefficient
FR	= fineness ratio
k	= number of cubic polynomials in spline fit
K	= body form factor

L	= length
M	= Mach number
P	= pressure
R	= radius
Re_L	= Reynolds number per unit length
s	= variable of integration along cross section contour
S	= cross sectional area
X	= independent parameter, axial location
β	= Prandtl-Glauert compressibility correction
ϕ	= coordinate transformation variable
θ	= nose terminal angle
μ	= Mach angle
ξ	= integration variable
Subscript	

B	= base
cr	= critical
exp	= based on experiment
min	= minimum value
ref	
ref	= reference quantity
wet	= wetted area
∞	= freestream condition

INTRODUCTION

The majority of the work described in this paper details a method for applying the wave drag area rule to axisymmetric bodies with arbitrary moldlines. Current preliminary design techniques for determining transonic wave drag are based on design charts for a few commonly used shapes. Often times, the designer is forced away from these shapes by packaging constraints, manufacturing processes, etc.. Thus, the effective design of tactical missiles requires knowledge of the basic

* Engineer, Member AIAA

** Senior Engineer, Member AIAA

This paper is declared a work of the U.S. Government and is not subject to copyright protection in the United States.

aerodynamic effects of a minor change in nose shape. A simple analytic method which accurately predicts wave drag is needed to improve this aspect of the preliminary design process. A numerical application of the transonic area rule will fill this void.

The area rule concept is not new, yet its quantitative use seems to be limited. This in part may be due to the mathematical difficulties encountered during the actual implementation of the method. The primary purpose of this paper is to present a simple approach to the numerical implementation of the area rule for axisymmetric bodies. In addition, the accuracy of the method is validated with experimental data comparisons. For completeness, an empirical method for subsonic pressure drag prediction is included, along with a fairing technique between the subsonic and supersonic methods.

A physical explanation for the transonic area rule can be thought of in terms of wave propagation at the speed of sound. At $M_\infty = 1$, the Mach planes are normal to the body axis. All disturbances generated at a given axial location on a body are first felt at that same axial location. In fact, the effect of a disturbance should be approximately the same on all surfaces intersected by that Mach plane. Assuming now that flow disturbances are a result of changes in the surface contour (and thus cross-sectional area), we have a direct link between the cross-sectional area development along a configuration and its wave drag.

In 1956, Richard Whitcomb (Reference 1) documented a series of famous experiments in which he measured the wave drag on various bodies of revolution with and without wings. Whitcomb's results indicated that body contouring could be used to reduce the wave drag on wing-body configurations.

The qualitative implications of the transonic area rule are well known. However, its quantitative roots in slender body theory and its extension to supersonic flow are less familiar, but equally as important. Reference 2 presents a complete derivation of Ward's drag formula based on slender body theory. It is applicable to slender, pointed bodies. If we assume that a

body cross-section is not varying axially at the base of the body (i.e. $S'(L) = 0$), and we neglect base drag, the slender body theory expression for inviscid drag reduces to

$$C_{Dw} = -\frac{1}{2\pi S_{ref}} \int_0^L \int_0^L S''(x)S''(\xi) \ln(x-\xi) dx d\xi \quad (1)$$

which represents the drag contribution solely due to wave formation. Inspection of Equation (1) points out two important features of wave drag. First, it is only a function of the cross-sectional area distribution. This fact was noted earlier during the discussion of Whitcomb's experimental investigation. Second, the slender body theory expression for wave drag is not an explicit function of freestream Mach number. However, as presented by Jones (Reference 2), the slender body theory expression for wave drag can be applied at supersonic Mach numbers if the cross-sectional area is taken to be the intersection of the body and an oblique plane, $S_\alpha(x)$, at the appropriate Mach angle. For axisymmetric bodies, $S_\alpha(x)$ needs only to be calculated once at each axial location along the body.

ANALYTIC DESCRIPTION

Supersonic Pressure Drag

Supersonic wave drag is calculated using a numerical application of the area rule. This states that the zero-lift wave drag is dependent upon the axial development of cross-sectional areas calculated along oblique planes. The oblique planes were oriented at the Mach angle with respect to the body centerline as shown in Figure 1. The axial development of the oblique areas are used in the evaluation of the drag integral. The parasitic pressure drag can be neglected if the local slope of the nose contour is small. As the local slopes increase, as with decreasing fineness ratio, this assumption is no longer valid.

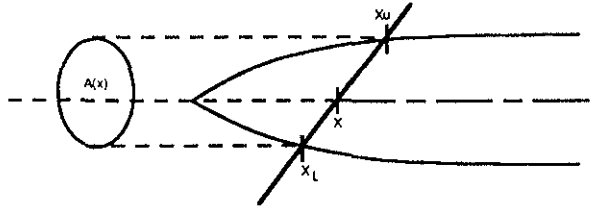


Fig. 1 Frontal Projection of Area Cut by Mach Plane.

As suggested by Nelson and Welsh (Reference 3), it is convenient to represent $S'(x)$ in Equation (1) in terms of a Fourier sine series. The coefficients of the series are

$$a_n = \frac{2}{\pi} \int_0^{\pi} \frac{dS}{dx} \sin n\phi d\phi \quad (2)$$

where

$$\phi = \cos^{-1} \left(\frac{2x}{L} - 1 \right) \quad (3)$$

The area derivative represented by $S'(x)$ corresponds to the frontal projection of each oblique plane cut by the Mach line, as shown in Figure 1. The frontal projection of the area can be calculated as

$$S(x) = \frac{2}{\beta^2} \int_{x_l}^{x_u} \sqrt{\beta^2 R^2(x) - (x-x_0)^2} dx \quad (4)$$

The limits of integration, x_u and x_l are implicit functions of the axial location x_0 , and are determined iteratively. For the numerical application, the computer program reads in the r

vs. x geometry data and applies a cubic spline fit to obtain an analytic representation of $S(x)$. At a given axial location, x_0 , the upper (and lower) intersection of the Mach line and nose radius contour is calculated. This is done by evaluating the spline fit at various values of x until the x -station at which the Mach line and nose moldline intersection is found. A cylindrical centerbody must be added for $M_\infty=1$ to allow the lower Mach line intersection to reach the base of the nose. It is assumed that the constant radius centerbody does not contribute to the wave drag.

Equation (4) is solved using Simpson's integration algorithm. A second cubic spline is used to fit the oblique area distribution, $S(x)$, with piecewise cubics as shown in Equation (5).

$$\begin{aligned} S_1(x) &= c_{01} + c_{11}x + c_{21}x^2 + c_{31}x^3 \\ S_2(x) &= c_{02} + c_{12}x + c_{22}x^2 + c_{32}x^3 \\ &\vdots \\ S_{n-1}(x) &= c_{0,n-1} + c_{1,n-1}x + c_{2,n-1}x^2 + c_{3,n-1}x^3 \end{aligned} \quad (5)$$

$S_i(x)$ represents the polynomial fit between x_i and x_{i+1} . The quantity of interest, $S'(x)$, is found analytically by differentiating the cubic polynomials as shown in Equation (6).

$$\begin{aligned} S'_1(x) &= c_{11} + 2c_{21}x + 3c_{31}x^2 \\ S'_2(x) &= c_{12} + 2c_{22}x + 3c_{32}x^2 \\ &\vdots \\ S'_{n-1}(x) &= c_{1,n-1} + 2c_{2,n-1}x + 3c_{3,n-1}x^2 \end{aligned} \quad (6)$$

The spline fit of the area distribution can then be used to determine the Fourier coefficients in Equation (2). A significant advantage of using cubic splines to represent the oblique area distribution is apparent when solving Equation (2) to determine the Fourier coefficients. Equation (6) can be substituted directly into Equation (2), using Equation (7) to express x in terms of ϕ .

$$x = \frac{L}{2}(1 + \cos \phi) \quad (7)$$

By collecting terms and integrating, the Fourier coefficients can be expressed algebraically as

$$a_n = \int_0^\pi S'(\phi) \sin n\phi d\phi = \sum_{n=1}^k \left[\begin{aligned} & \left(c_1 + c_2 L + \frac{3}{4} c_3 L^2 \right) \sin n\phi \\ & + \left(c_2 L + \frac{3}{2} c_3 L \right) \sin \phi \cos \phi \\ & + \frac{3}{4} c_3 L^2 \sin \phi \cos^2 \phi \end{aligned} \right] \quad (8)$$

The constant, k, represents the number of cubic polynomials in the spline fit. The solution for C_{Dw} is then simply determined by summing the Fourier coefficients as shown below. The series is shown to be adequately converged in Reference 3 using the first 24 terms.

$$C_{Dw} = \frac{\pi}{4 S_{ref}} \sum_{n=1}^{24} n a_n^2 \quad (9)$$

Subsonic Pressure Drag

Parasitic drag is classified as that which is independent of lift. This drag consists of skin friction drag and form drag. The subsonic form drag is directly related to the boundary layer development along the body. Thus, knowing the friction drag for the body, the subsonic form drag can be correlated with the skin friction coefficient and the body fineness ratio as shown in Equation (10).

$$C_{D_{po}} = \frac{K C_f S_{wet}}{S_{ref}} \quad (10)$$

The body form factor, K, is based on the fineness ratio of the whole body. This empirical factor as used in this program is determined from Figure 2 as given in Reference 4. Method accuracy has not been verified for body fineness ratios less than 5. At high subsonic Mach numbers, the body pressure distribution varies according to the Prandtl-Glauert rule. This rule and its effect on form drag are reflected in Equation (11).

$$C_{D_p} = \frac{C_{D_{po}}}{\sqrt{1 - M_\infty^2}} \quad (11)$$

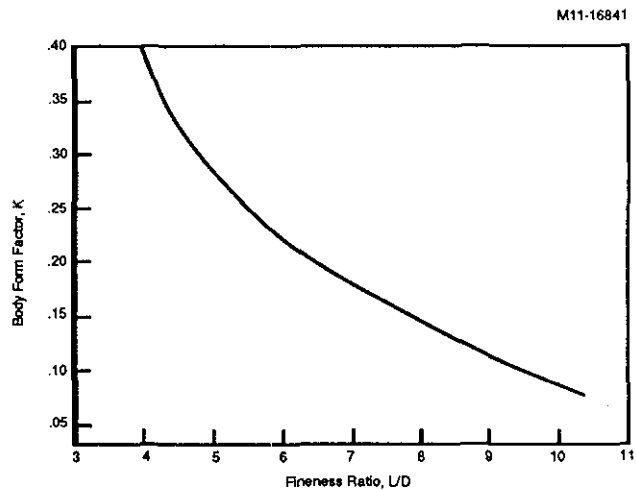


Fig. 2 Body Form Factor Empirical Correlation (Ref. 4).

The skin friction coefficient can be calculated using a variety of popular techniques. Perhaps the simplest method for preliminary design is the familiar result of turbulent integral boundary layer theory shown in Equation (12).

$$C_f = \frac{0.072}{Re_L^{0.2}} \quad (12)$$

Transonic Pressure Drag

The transonic region is characterized by the significant drag rise that occurs due to shock wave formation. A third order polynomial is

used to smoothly model the drag rise between the subsonic and supersonic regions. The transonic region is assumed to begin at the value of M_∞ at which the local Mach number first reaches unity and end at a value of $M_\infty = 1.2$. The magnitude and slope of the subsonic and supersonic pressure drag curves are calculated at these Mach numbers and are used in the third order curve formulation.

A method for predicting the critical Mach number for different nose shapes was developed to better define the onset of the transonic drag rise. This method consists of a correlation between the fineness ratio and the angle between the nose and centerbody juncture for a given nose shape.

A database consisting of pressure distributions about axisymmetric bodies was constructed with the use of a code which represents bodies of revolution as axial line singularities (Reference 5). The quantity of interest was C_{pmin} , which occurs at the nose-centerbody juncture. Four nose shapes with varying fineness ratios were evaluated. They consisted of tangent-ogive, 1/2 power law, 3/4 power law and conical nose shapes with fineness ratios from 2.0 to 10.0.

Figures 3 and 4 suggest that a simple relationship between fineness ratio and terminal angle of the nose could be found. Figure 3 shows the comparison of C_{pmin} versus fineness ratio. Figure 4 shows the linear behavior of C_{pmin} with the nose terminal angle. Based on the curves shown in Figure 3, it was felt that a linear curve fit for each of the nose shapes could be found. Figure 5 illustrates the linear relationship established between C_{pmin} and the fineness ratio for the four nose shapes. Equation (13), which describes Figure 5, is given below. C_{pmin} is determined for axisymmetric nose shapes as a function of fineness ratio and nose terminal angle.

$$C_{pmin} = \left\{ 10FR \left[0.22 - 0.13 \left(\frac{\theta}{\theta_{cone}} \right)^{0.75} \right] \right\}^{-1.25} \quad (13)$$

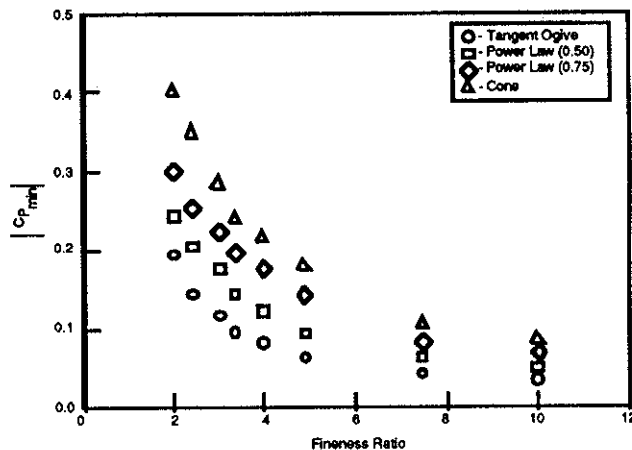


Fig. 3 Nose Shape and Fineness Ratio Effects on Minimum Incompressible Surface Pressure Coefficient.

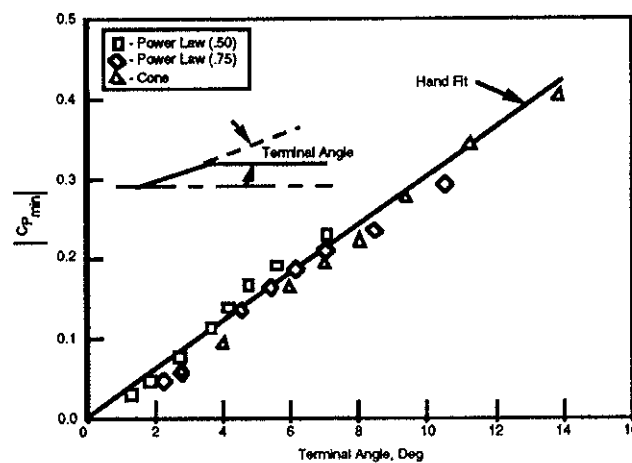


Fig. 4 Nose Shape and Terminal Angle Effects on Minimum Incompressible Surface Pressure Coefficient.

The critical Mach number is calculated from a graphical method presented in Reference 6. A curve fit representing the C_{pmin} vs. Mach number curve was determined and is shown in Equation (14).

$$M_{cr} = \exp(0.521 |C_{pmin}|^{0.645}) \quad (14)$$

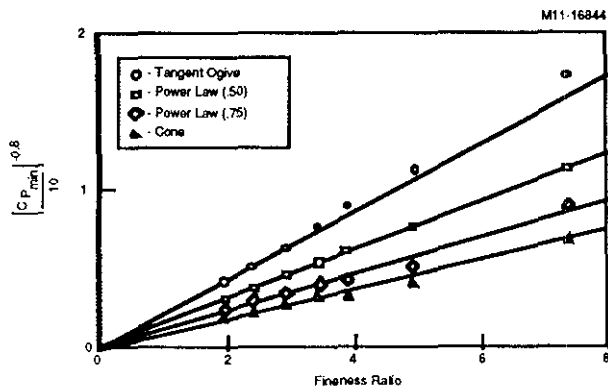


Fig. 5 Linear Correlation of Minimum Incompressible Surface Pressure Coefficient with Fineness Ratio and Nose Shape.

The Mach number at which the flow becomes locally sonic is now known and can be used to calculate the pressure drag at transonic speeds. The transonic range is assumed to include Mach numbers from the critical Mach number through $M_\infty = 1.2$.

The process by which the pressure drag at a Mach number within this range is calculated, is as follows. In order to describe a third order curve, the values of the pressure drag and its derivatives are found at the limiting Mach numbers of the transonic range. The supersonic pressure drag is calculated at $M_\infty = 1.2$ as described in the supersonic description. The pressure drag is computed again at a Mach number of 1.3 and the slope is determined using a finite difference. The same procedure is used subsonically to obtain the final two boundary conditions. Once the four boundary conditions are known, the polynomial describing the transonic drag rise is calculated.

PROGRAM RESULTS

Calculated results for different nose shapes are presented against a collection of experimental nose pressure drag data in Figures 6 through 8. These figures illustrate the strengths and limitations of the code. References 7 through 9 contain the experimental data used for the comparisons.

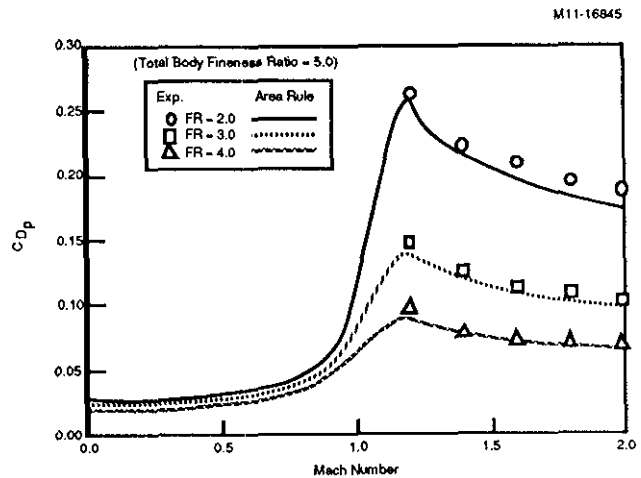


Fig. 6 Pressure Drag Predictions on Fineness Ratio 2, 3, and 4 Conical Noses.

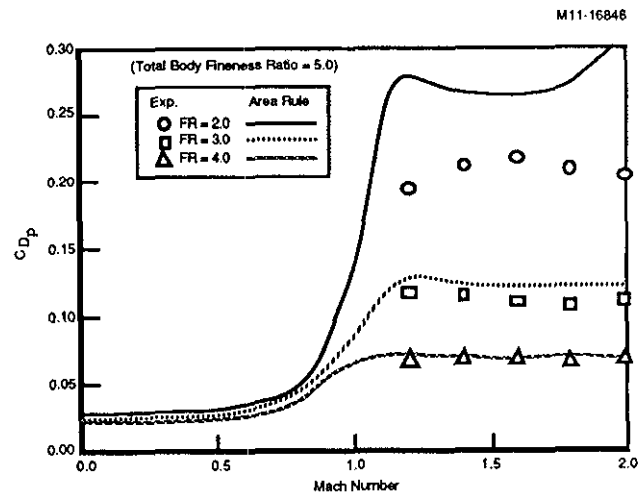


Fig. 7 Pressure Drag Predictions on Fineness Ratio 2, 3, and 4 Tangent Ogive Noses.

Values for the supersonic wave drag are good for high to moderate nose fineness ratios. Figure 6 illustrates the excellent agreement with experimental data for conical nose shapes. Since the pressure term is being ignored, wave drag predictions for conical nose shapes were expected to be accurate. The assumption of constant pressure along the body is good for bodies without high local slopes and no discontinuities. The only discontinuity on the conical nose shapes is at the nose-cylinder juncture.

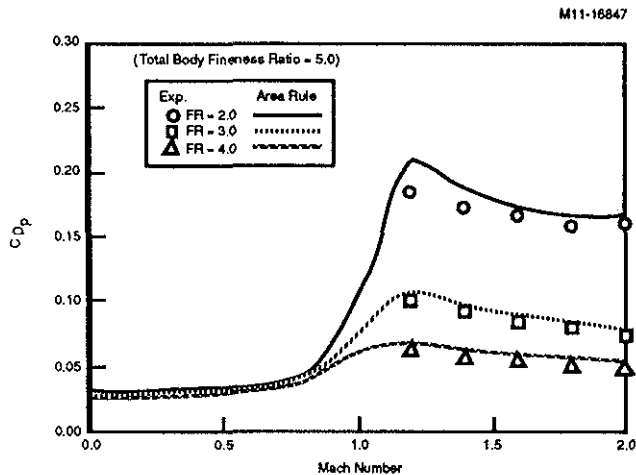


Fig. 8 Pressure Drag Predictions on Fineness Ratio 2, 3, and 4 Power Series ($n=0.75$) Noses.

The results for some nose shapes which have a fineness ratio lower than 2.75 show a different trend than the experimental data as shown in Figure 7. The prediction for the fineness ratio 2.5 tangent-ogive nose begins showing a different trend for Mach numbers above 1.5. This is not surprising since the area rule formulation is based upon slender body theory. We are trying to analyze a shape which has large local slopes at the nose, yet neglecting pressure changes along the body.

Figures 6, 7 and 8 all illustrate the power of the numerical method for determining the supersonic pressure drag for higher fineness ratio bodies. Wave drag predictions for nose shapes with fineness ratios greater than 2.75 can be expected to agree with experimental data.

The subsonic results agree both qualitatively and quantitatively with experimental data. The assumption of a turbulent boundary layer and the use of a body form factor is an accepted method for predicting subsonic pressure drag. The transonic results capture the drag rise and follow experimental trends.

For applications where quantitative accuracy is of prime importance, the area rule calculations were modified with a fineness ratio

and volume correction. Figures 6 through 8 show that as nose fineness ratio increases, the results from the current method are in better agreement with experimental data. This was expected with linear theory. In order to produce better results at lower fineness ratios, a correlation based on the volume and fineness ratio of the nose was determined. Establishing the lowest volume non-concave nose for a given length and diameter, a cone, as the baseline; a correlation factor was computed. Tangent ogive forebody shape is used as the highest volume body. The tangent ogive data was plotted against experimental data and a correction factor was determined for three different fineness ratios. The correction factor is determined by a linear interpolation between the volume and fineness ratio extremes. Figure 9 illustrates the correction factor as a function of nose volume and fineness ratio.

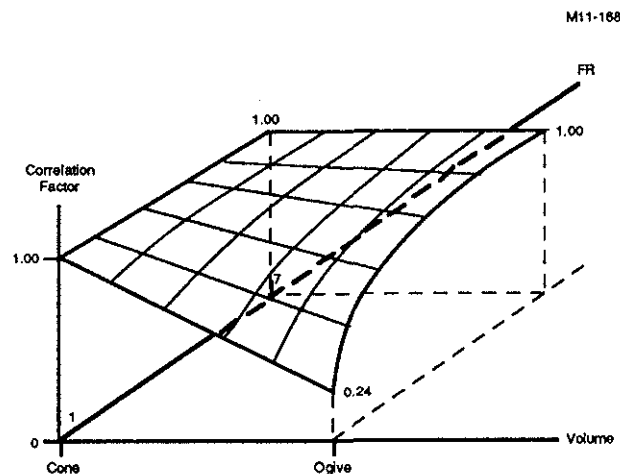


Fig. 9 Area Rule Correlation with Experimental Data.

Improved results are realized with the correlation as shown in Figures 10 and 11. The correlation allows for a better quantitative agreement with experimental data without foregoing the good qualitative trends presented earlier.

CONCLUSIONS AND RECOMMENDATIONS

The results for three common nose shapes are presented against experimental data. The

program can predict pressure drag over a Mach number range from 0 to 2. Good pressure drag predictions are shown for bodies with nose fineness ratios greater than 2.5 and total body fineness ratios greater than 5. The magnitudes and trends shown by the program methodology are well suited for preliminary design.

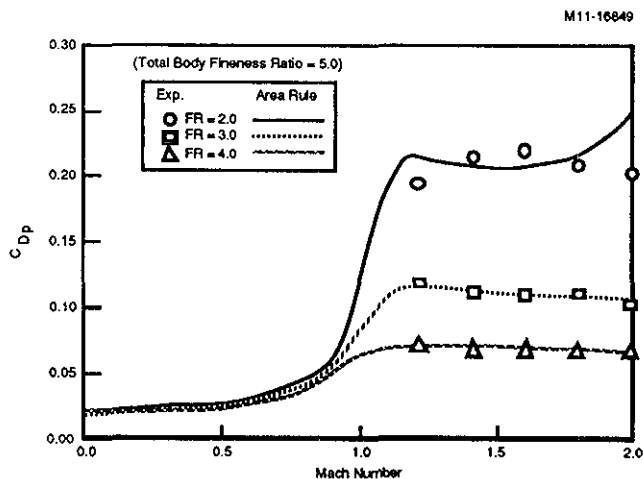


Fig. 10 Correlated Pressure Drag Predictions on Tangent Ogive Noses.

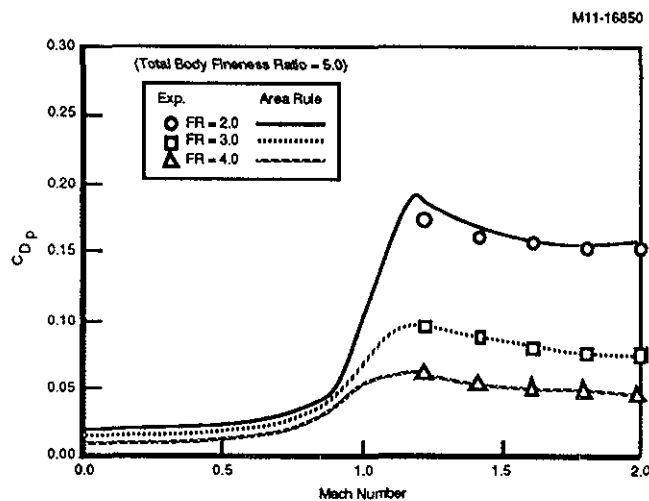


Fig. 11 Correlated Pressure Drag Predictions on Power Series ($n=0.75$) Noses.

The ability to analyze the pressure drag of axisymmetric bodies with arbitrary moldlines is realized with this program. The addition of a method to calculate the critical Mach number enabled accurate transonic drag rise trends to be predicted. The program enhancement correlation increases the quantitative accuracy while preserving the qualitative trends. The code's utility as a preliminary design tool is also well suited for arbitrary shapes which can be represented as an equivalent body of revolution. The (x,r) coordinates can then be entered just as they were for axisymmetric nose shapes with arbitrary moldlines.

REFERENCES

1. Whitcomb, R.T., "A Study of the Zero-Lift Drag Rise Characteristics of Wing-Body Combinations Near The Speed of Sound," NACA TR 1273, 1956.
2. Jones, R.T., "Theory of Wing-Body Drag at Supersonic Speeds," NACA TR 1284, 1957.
3. Nelson, R.L., Welsh, C.J., "Some Examples of the Applications of the Transonic and Supersonic Area Rules to the Prediction of Wave Drag," NASA TN D-446, September, 1960.
4. Shevell, R.S., Fundamentals of Flight, Prentice-Hall, Englewood Cliffs, N. J., 1983. CHAPT 13
5. Hemsch, M.J., "An Improved, Robust, Solution Method for Representation of Bodies of Revolution by Axial Line Singularities," AIAA Paper No. 89-2176, 1989.
6. McCormick, B.W., Aerodynamics, Aeronautics, and Flight Mechanics, John Wiley and Sons, New York, 1979.
7. Stoney, W.E., "Transonic Drag Measurements of Eight Body-Nose Shapes," NACA RM L53K17, February, 1954.

8. Butler, C.B., Sears, E.S., Pallas, S.G.,
"Aerodynamic Characteristics of 2-, 3-,
and 4-Caliber Tangent-Ogive Cylinders
with Nose Bluffness Ratios of 0.00, 0.25,
0.6, and 0.75 at Mach Numbers from 0.6
to 4.0," AFATL-TR-77-8, January, 1977.
9. Perkins, E.W., Jorgensen, L.H., Sommer,
S.C., "Investigation of the Drag of Various
Axially Symmetric Nose Shapes of
Fineness Ratio 3 for Mach Numbers from
1.24 to 7.4," NACA R-1386, August,
1952.